New quantitative methods of ventricular repolarization analysis in patients with left ventricular hypertrophy

Alexandru D. Corlan, Luigi De Ambroggi*

*Cardiology Research Unit, University Hospital, Bucharest, Romania, *Department of Cardiology, Istituto Policlinico San Donato, University of Milan, Milan, Italy*

Key words:
Left ventricular hypertrophy; Principal component analysis; Repolarization heterogeneity; Surface potential mapping.

Background. **Left ventricular hypertrophy (LVH) is accompanied by specific changes in ventricular electrophysiology, which are potentially arrhythmogenic. Nevertheless, the electrocardiographic diagnostic signs for LVH have a relatively low predictive power for arrhythmic events and sudden death. We thought that other parameters derived from the surface ECG, not apparent at visual inspection, might be detected by specific analysis of electrocardiographic digital recordings. The purpose of our work was to analyze the surface distribution of repolarization potentials and search for subtle alterations not revealed by the usual electrocardiographic processing, which are likely to reflect ventricular repolarization heterogeneity.**

Methods. **Body surface potential maps were recorded from 62 chest leads in 16 patients with LVH due to aortic stenosis and in 35 normal subjects. By applying a principal component analysis of the ST-T waves, we computed the similarity index. The value of the similarity index is inversely proportional to the variability of T wave morphology and a low value is considered a marker of repolarization heterogeneity.**

Results. **The similarity index was significantly lower in LVH patients than in normals both in 62 leads (0.73 – 0.067 vs 0.77 – 0.044, p = 0.03) and in 12 unipolar leads (V_1-V_8, V_{3R}, VR, VL, VF) extracted from the map (0.77 – 0.075 vs 0.81 – 0.045, p = 0.03). Moreover, we computed the late repolarization deviation index , which quantifies the instantaneous variations of surface potential distribution from peak to end of the T wave. This index was significantly higher in LVH patients than in controls (in 62 leads 0.07 – 0.05 vs 0.028 – 0.016, p = 0.005; in 12 leads 0.064 – 0.052 vs 0.024 – 0.020, p = 0.008).**

Conclusions. **The values of similarity index and of late repolarization deviation index found in LVH patients suggest a higher than normal degree of repolarization heterogeneity, not detected by the usual electrocardiographic analysis. Since both indices maintained statistical significance when calculated on the 12 leads derived from our map lead system, they could be reliably computed from digital recordings of the 12 conventional leads.**

(Ital Heart J 2000; 1 (8): 542-548)

Dr. A.D. Corlan worked in the Istituto Policlinico San Donato, Department of Cardiology, as international resident funded by the E. Malan Cardiovascular Center scholarship.

Received April 20, 2000; revision received July 5, 2000; accepted July 17, 2000.

Address:

Dr. Luigi De Ambroggi

Cattedra di Cardiologia
Istituto Policlinico
San Donato
Via Morandi, 30
20097 San Donato
Milanese (MI)
E-mail: Luigi.DeAmbroggi@unimi.it

Introduction

Left ventricular hypertrophy (LVH) is associated with increased risk of malignant arrhythmias and sudden cardiac death[1,2]. In fact, LVH is accompanied by specific changes in ventricular electrophysiology at the cell and tissue level[3-5], which are potentially arrhythmogenic. Nevertheless, the electrocardiographic diagnostic signs for LVH have a relatively low predictive power for arrhythmic events and sudden death[1]. QT interval dispersion, late potentials, heart rate variability, and Lown class have also been explored for risk stratification in LVH patients, with varied results[6-9]. We thought that other parameters derived from the surface electrocardiogram (ECG), not apparent at visual inspection, might be detected by specific analysis of electrocardiographic digital recordings. We focused on repolarization analysis since it is generally accepted, on the basis of experimental data[10,11], that repolarization inhomogeneity facilitates the reentry circuits leading to the development of ventricular arrhythmias. This can happen in the hypertrophied myocardium.

The purpose of the present work was to analyze repolarization potentials on the entire chest surface to identify differences between normal and LVH electrocardiographic digital recordings, which are likely to reflect repolarization heterogeneity, that cannot be derived from classical LVH diagnostic indices.

Methods

Study population. We recorded body surface potential maps in 16 patients (8 males, 8 females, aged 68 – 13 years), with valvular aortic stenosis documented by echocardiographic examination (mean transaortic gradient > 45 mmHg). LVH was determined by echocardiographic measurements of the interventricular septum and posterior wall thickness, and ventricular mass according to the recommendations of the American Society of Echocardiography. Ventricular mass index was 182 – 51 g/m^2 in our LVH group.

The ECG showed QRS voltage criteria positive for the diagnosis of LVH ($S_{V1} + R_{V5}$ or $R_{V6} > 35$ mm) in 14 patients and ST-T abnormalities (ST segment depression, flat or negative T waves in precordial leads) in 12 patients. In 2 cases the QRS amplitude was within normal limits, but ST-T alterations were present. No patient had experienced episodes of severe ventricular arrhythmias (sustained or non-sustained ventricular tachycardias). Patients with bundle branch block and atrial fibrillation were excluded. All patients underwent coronary angiography, that showed no critical (50%) coronary stenosis in any patient.

Thirty-five healthy subjects (25 males, 10 females, aged 33 – 10 years), without any history of symptoms due to cardiac disturbances, and with a normal standard ECG, were studied as controls. Moreover, we considered 159 normal subjects older than 30 years as a separate control group, whose surface potential map recordings were made available by Dr. F. Kornreich from Vrije Universiteit of Brussels (VUB, Belgium). As these maps were recorded using 120 leads, a transformation procedure[12] from 120 to 64 lead system was applied before analyzing the data.

Body surface potential map recording. The equipment used has already been described in a previous paper[13]. Briefly, we used a 64-channel mapping system, with the irregular lead array configuration originally adopted by SippensGroenewegen et al.[14] (Fig. 1), with a sampling rate of 1000 Hz and an amplitude resolution of 16 bits. All the recordings were performed with the subject in the supine position. One low-noise cardiac cycle was selected in each recording and baseline correction was performed on that segment.

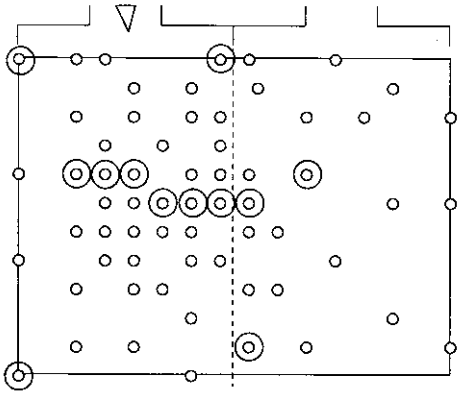

Figure 1. *Schematic drawing showing the lead system used with the position of 62 electrodes on the anterior* (left half) *and posterior* (right half) *chest surface. The leads selected for the 12-lead subset are circled.*

The QRS onset and end, as well as the end of the T wave were identified manually from the root mean square (RMS) signal of the map (the signal which is the root mean square of the amplitudes in each of the leads). The peak of the T wave was automatically computed as the instant during the ST-T interval where the RMS signal had the maximal value. The last 1 ms sample after this moment, where the RMS still had a value > 50 μV, was taken as the automatically detected end of the T wave and was the estimation used during later processing.

Integral maps. The QRS, ST-T and QRST integral maps were obtained by calculating at each lead point the algebraic sum of all instantaneous potentials of a given interval multiplied by the sampling interval. The values in millivolts × milliseconds were plotted on the diagram representing the chest surface, and the isointegral contour lines were drawn. Group mean maps were calculated using respective mean values at each lead point.

Similarity index. Each of the ST-T intervals was resampled at 20 ms, resulting in N = (STT duration)/20 ms samples in each recording. For each recording we performed a principal component analysis of the matrix with N variables (sets of potentials at each of the resampling points) of 62 values. The result was a set of N eigenvectors and N eigenvalues for each recording.

The amount of the body surface potential variation described by the first principal component is expressed as the first eigenvalue. The extent to which, after subtracting the first principal component, the signal is described by the second principal component, is expressed by the second eigenvalue, and so on[15].

We defined the similarity index (SI) as the first eigenvalue divided by the sum of all eigenvalues[13,16].

The same analysis was repeated in a subset of 12 leads from the set of 62 available (Fig. 1). The 12 leads used roughly correspond to: V_1 to V_6, V_8, V_{3R}, V_{4R}, VR, VL, VF. When a distinction is necessary, SI is denoted SI_{62} if computed on 62 leads and SI_{12} if computed on 12 leads.

Early and late repolarization deviation indexes. At visual inspection the distribution of the potentials on the body surface during repolarization is generally constant in time, apart from changes in amplitude. In other words, during repolarization the amplitude of the potentials on the surface increases and decreases overall, but the relative amplitudes on one lead with respect to another are generally unchanged (Fig. 2). The early repolarization deviation index (ERDI) and late repolarization deviation index (LRDI) are numerical indices which describe deviations from this behaviour during repolarization, from the J point to the T peak and from the peak to the end of the

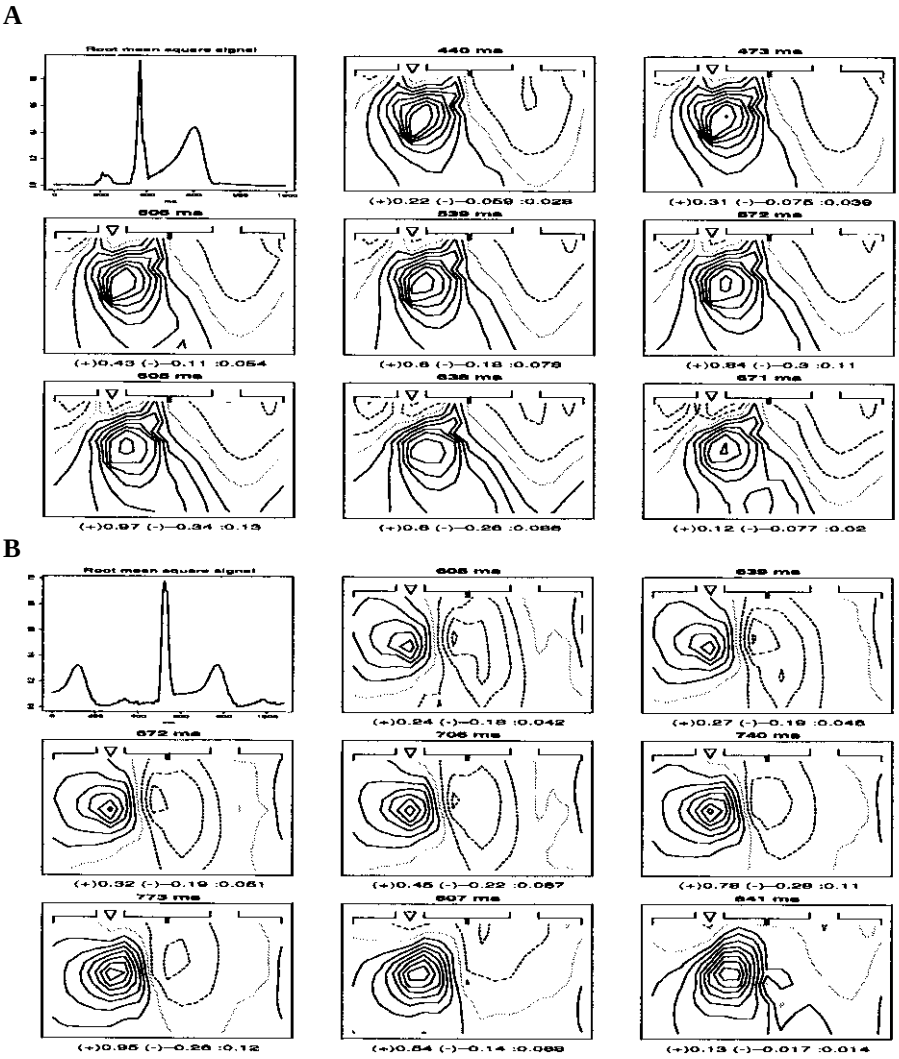

Figure 2. *Instantaneous maps of potential distribution during ventricular repolarization in a normal subject* (A), *and in a patient with left ventricular hypertrophy* (B). *At the top of each map the number in milliseconds indicates the time from the beginning of the recording, reproduced in the first* (top, left) *box of the series. Isopotential lines with positive values are* continuous, *those with negative values are* dashed*; the zero line is* dotted. *The isopotential line step is adjusted so that there are 10 isopotential lines in every map (so changes in the relative amplitude can be easily seen).*

T wave, respectively. The potential distribution at the peak of the T wave (peak-T map) was taken to represent the most well defined distribution of the repolarization potentials. For each instant during the cardiac cycle we computed the Pearson correlation coefficient between the potentials of each lead at that instant and the potentials of the same leads at the peak-T map. This value is 1.0 if at that instant the map has identical distribution with the peak-T map (apart from the amplitude), -1.0 when it is exactly opposite (again, apart from the amplitude) and 0.0 when it shows no resemblance. Subunit values measure the extent of the resemblance between the instantaneous map and the peak-T map. We called this function of time quantity the instantaneous correlation with the peak-T map (ICPTM).

The expected normal behavior during repolarization is to have an ICPTM near to 1.0 level during the whole repolarization. Some cases, like the one in figure 3A, are close to this ideal. Some others, like the one in figure 3B, show a more or less important deviation from it. In order to quantify the deviations from the J point to T peak and from T peak to T end, we divided the area between the ICPTM signal and the 1.0 line by the duration of the respective intervals. We called these values ERDI and LRDI.

Statistical analysis. Data are summarized as sample mean – SD, where not stated otherwise. The Student s t test was used to compare means of quantitative variables obtained in two data sets.

The Pearson s product-moment correlation coefficient was used to estimate the correlation coefficient between different variables measured in the same group of patients, when not specified otherwise. When the plot of the pairs of values did not show a binormal distribution the Spearman coefficient was used.

The programs used for the generic processing of the recordings (beat extraction, baseline and lead correction),

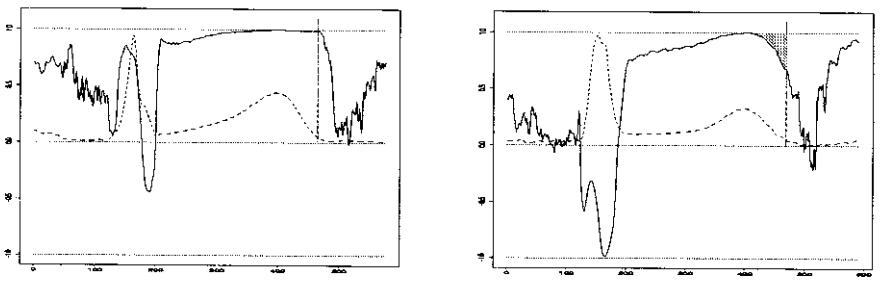

A **B**

Figure 3. *Normal subject* (A), *patient with left ventricular hypertrophy* (B). *Correlation of the instantaneous maps with the map related to the peak of the T wave. The* dotted line *represents the root mean square of the 62 leads. The* continuous line *is the instantaneous correlation with the peak-T map signal. The end of the T wave is indicated by the* vertical bar. *Compared to* A, *in* B *there is a clear decay of the instantaneous correlation with the peak-T map during the descending limb of the T wave. The late repolarization deviation index value is given by the gray area divided by the interval between the peak and the end of the T wave.*

and for the analyses peculiar to this paper were developed in our laboratory. The specific analysis programs were based on the R statistical package (an implementation of the S-Plus language). Computations were done on a P90 computer running Debian Linux v1.3.

Results

The classical signs of LVH in the standard ECG (increased QRS voltage and ST-T changes) are reflected on body surface maps as: 1) increased amplitude of the QRS integral map and of the ST-T integral map (Table I), 2) relatively low amplitude of the QRST integral map, due to the cancellation between the depolarization and repolarization potentials, 3) opposing aspects of the QRS and ST-T integral maps (Fig. 4D, E).

In all 16 patients the ST-T integral maps showed an abnormal distribution of the values with a minimum located on the left mammary region and a maximum on the right. This distribution was roughly opposed to that of the QRS map (Fig. 4). The QRST integrals in LVH had a lower overall amplitude, especially in the regions of negativity on the back and on the upper right quarter of the thorax. The shape and position of the zero isointegral line showed little change from normals (Fig. 4).

The opposition of the repolarization over most of the body surface is also reflected by the changes in the ICPTM line (Fig. 3). In normals, during the QRS interval, it shows an initial positive correlation with peak-T map, which extends for the first two thirds of the depolarization and a smaller final negative correlation (Fig.

Table I. Mean values – SD of various indices in the control and left ventricular hypertrophy (LVH) groups.

	Normals	LVH	p
SI_{62}	0.77 – 0.044	0.73 – 0.067	0.027
SI_{12}	0.81 – 0.045	0.77 – 0.075	0.030
$ERDI_{62}$	0.21 – 0.24	0.13 – 0.10	0.1
$ERDI_{12}$	0.20 – 0.23	0.11 – 0.12	0.23
$LRDI_{62}$	0.028 – 0.016	0.070 – 0.050	0.005
$LRDI_{12}$	0.024 – 0.020	0.063 – 0.052	0.008
QRS integral (mVms)	69.3 – 26.2	164.1 – 68.1	0.00005
QRST integral (mVms)	148.2 – 56.2	104.8 – 38.9	0.003
ST-T integral (mVms)	130.1 – 49.8	186.5 – 96.7	0.041

$ERDI_{62}$, $ERDI_{12}$ = early repolarization deviation index computed in 62 and in 12 leads, respectively; $LRDI_{62}$, $LRDI_{12}$ = late repolarization deviation index in 62 and in 12 leads, respectively; SI_{62}, SI_{12} = similarity index in 62 and in 12 leads, respectively; QRS, QRST, ST-T integral = positive peak to negative peak difference (in millivolts × milliseconds) in the respective integral map.

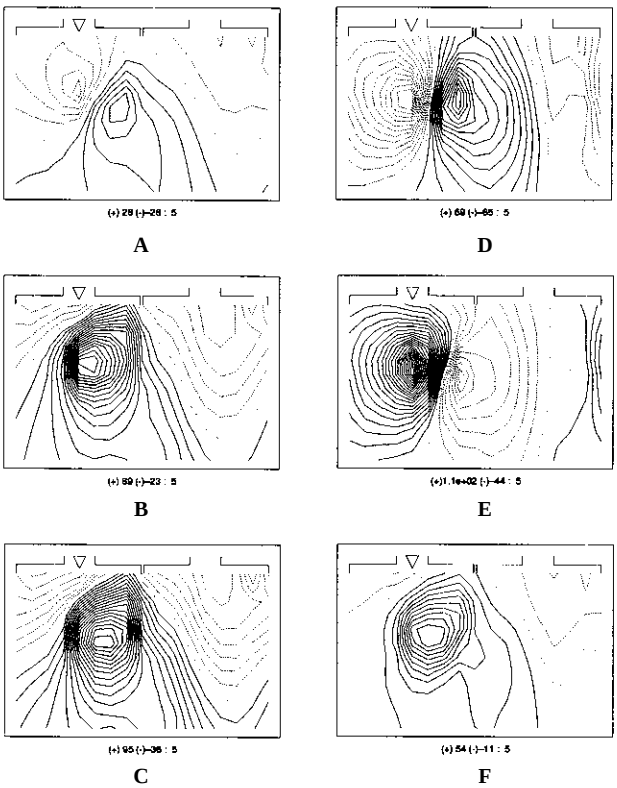

A **D** **B** **E** **C** **F**

Figure 4. *Mean QRS, ST-T and QRST integral maps in the control group* (A, B *and* C, *respectively) and in the group with left ventricular hypertrophy* (D, E, F). *Isointegral line step is 10 mVms; the* continuous *isointegrals represent positive values whereas the* dotted *ones represent negative values.*

3A). In LVH patients the ICPTM typically shows a deep inverse correlation with the peak of the T wave during the whole QRS interval (with the exception of a short period at the beginning of the QRS in some cases) (Fig. 3B).

Similarity index, and early and late repolarization deviation indexes. The SI was significantly lower in aortic stenosis than in normal subjects (Table I), both in the 62 and 12 lead recordings.

The ERDI computed in 62 and 12 leads was not significantly different in LVH and in control groups.

The LRDI was significantly higher in aortic stenosis than in normals (Table I) in 62 and 12 lead recordings. The $LRDI_{62}$ was not significantly correlated with SI_{62} ($r = 0.404$, $p = NS$) in LVH patients.

SI, ERDI, and LRDI were also computed in the 159 VUB recordings of normal subjects after appropriate lead system transformation[12]. No significant difference was found between our subjects and those of the VUB (Table II). The comparison of SI, ERDI, LRDI in the LVH group and in the VUB normals substantially confirmed the results obtained using our smaller control group (Table II).

Table II. Mean values – SD of some indices in our control group (Na) and in the group of the Vrije Universiteit of Brussels (Belgium) of 159 normal subjects (Nb).

	Na	Nb	p (Na vs Nb)	p (Nb vs LVH)
SI_{62}	0.77 – 0.04	0.76 – 0.06	0.38	0.05
$ERDI_{62}$	0.21 – 0.24	0.17 – 0.12	0.33	0.23
$LRDI_{62}$	0.028 – 0.016	0.030 – 0.029	0.43	0.007

Abbreviations as in table I.

Correlations with other variables. SI_{62} showed a weak correlation with the QT interval duration (Spearman $\rho = 0.5$, $p = 0.052$) and an inverse correlation with age ($\rho = -0.662$, $p = 0.01$) in the aortic stenosis group but not in the normal group ($\rho = -0.11$ and $\rho = -0.06$, respectively). It was not correlated with ventricular mass, ventricular mass index, body surface area, transaortic gradient or ventricular wall size. The logarithm of LRDI showed a weak correlation with ventricular mass index, at the limit of statistical significance ($r = 0.54$, $p = 0.058$).

Discussion

The mapping of repolarization potentials exhibited clearly abnormal patterns in patients with aortic stenosis. Specifically, the ST-T integral maps constantly showed a dipolar distribution of the positive and negative values contrary to that of the respective QRS integral maps. This was expected in patients with LVH, on the basis of the common electrocardiographic knowledge and of the findings of surface potential mapping previously reported[17-19].

The QRST integral maps mainly reflect the intrinsic repolarization properties and are thought to be largely independent of ventricular activation sequence[20,21]. A multipolar distribution on QRST integral maps has been related to local disparities of ventricular repolarization and thus to a cardiac state of vulnerability of arrhythmias[22-25]. In our study group only 2 patients showed a multipolar QRST map with one maximum and two separate minima. These findings could not be related to any clinical or functional characteristics, except the additional presence of a marked dynamic obstruction of the outflow tract in one patient.

In order to detect and quantify minor electrical disparities of repolarization not apparent from the visual inspection of the ST-T and QRST maps, we analyzed the morphology of all the recorded ST-T waves, using principal component analysis. We assumed that the more inhomogeneous the ventricular repolarization, the more complex the equivalent cardiac generator, giving rise to a more complex potential distribution at the body surface. On the other hand, the more uniform is the recovery process in the ventricles, the more dipolar the surface potential distribution. A smooth dipolar distribution of recovery potentials will result in ST-T waves with very similar shapes although of different amplitude and polarity. This condition will be reflected by a high value of the SI. Actually, in previous studies we found that SI was abnormally low in patients with or at risk for ventricular arrhythmias[13,16]. In patients with aortic stenosis SI was slightly but significantly lower, suggesting the presence of a degree of repolarization heterogeneity higher than in normals.

Correspondence between cellular events and electrocardiographic repolarization waves has recently been clarified by Yan and Antzelevitch[26,27] with simultaneous and direct recordings of transmembrane action potentials from intramural sites throughout the ventricular wall and a transmural ECG. Their findings demonstrated that the upslope of the T wave is largely due to the repolarization of the subepicardium, during which the amplitude of the subepicardial action potentials gradually decrease below that of the midmyocardial cells. The peak of the T wave corresponds to the complete repolarization of the epicardium, while the end of the T wave marks the completion of the repolarization of the M cells of the midmyocardium. Thus, during the downslope of the T wave the repolarization process is dispersed across the ventricular wall.

Although at the body surface T wave morphology is influenced not only by the transmural gradient, but also by other factors such as apico-basal gradient, inhomogeneity of the conducting medium, and geometry of the chest, we believed that a certain quantitative analysis of the repolarization potentials on the entire chest

could reveal signs of heterogeneity of the recovery process in the heart.

The ICPTM reflects the extent to which instantaneous body surface potential distribution resembles that at the peak of the T wave. We took the peak-T map as reference because at this time the repolarization potentials reach the highest amplitude that is when the pattern of the potential distribution is best defined. Moreover, the peak-T is theoretically a critical point, in that it corresponds to the moment separating the period when the ventricles are still more or less depolarized from the period when the subepicardial layers have been completely repolarized.

In our LVH patients the changes during early repolarization, as reflected by ERDI, were similar to those observed in our control group and in the larger VUB normal group. Then we focused on the analysis of the T peak-T end period, during which possible heterogeneities of repolarization should be more probably detected. This segment also includes the vulnerable period of the ventricles. The ICPTM departs progressively from the ideal 1.0 level during the downslope of the T wave, presumably reflecting the contribution of the inhomogeneous and late-to-repolarize regions of the subendocardium and midmyocardium to the surface potentials. The extent of this contribution is probably measured by the LRDI, i.e. by the mean value of the difference between ICPTM and 1.0 level during this period.

If the meaning we hypothetically attributed to SI and LRDI is correct, the values of these indices found in LVH patients suggest a degree of repolarization heterogeneity higher than normal. Thus, we could propose the two indices as markers of repolarization heterogeneity, and thus as candidate markers of vulnerability to arrhythmias in LVH. However, further studies in a larger population of LVH patients with and without occurrence of ventricular arrhythmias are warranted.

The present paper has the limit to be primarily a description of the methodology and does not report a demonstration of the clinical value of the findings. Nevertheless, it demonstrates that the proposed analysis of surface repolarization potentials provides novel, quantitative information on the complexity of the repolarization process, which cannot be obtained by the usual analysis of the ECGs performed in clinical practice.

Since we found that both SI and LRDI maintained their statistical significance even when calculated on 12 leads derived from our map lead system, we feel that the two indices could be also computed from digital recordings of the conventional 12-lead ECG. This could facilitate the validation of the proposed indices in a vast population of normal subjects and patients with various heart diseases, with and without ventricular arrhythmias, and eventually could provide additional information for the usual analysis of the ECG.

References

1. Levy D, Anderson KM, Savage DD, Balkus SA, Kannel WB, Castelli WP. Risk of ventricular arrhythmias in left ventricular hypertrophy: the Framingham Heart Study. Am J Cardiol 1987; 60: 560-5.
2. Haider AW, Larson MG, Benjamin EJ, Levy D. Increased left ventricular mass and hypertrophy are associated with increased risk for sudden death. J Am Coll Cardiol 1998; 32: 1454-9.
3. Cooklin M, Wallis WR, Sheridan DJ, Fry CH. Changes in cell-to-cell electrical coupling associated with left ventricular hypertrophy. Circ Res 1997; 80: 765-71.
4. Volders PG, Sipido KR, Vos MA, Kulcsar A, Verduyn SC, Wellens HJ. Cellular basis of biventricular hypertrophy and arrhythmogenesis in dogs with chronic complete atrioventricular block and acquired torsade de pointes. Circulation 1998; 98: 1136-47.
5. Tomaselli GF, Marban E. Electrophysiological remodeling in hypertrophy and heart failure. Cardiovasc Res 1999; 42: 270-83.
6. Bikkina M, Larson MG, Levy D. Asymptomatic ventricular arrhythmias and mortality risk in subjects with left ventricular hypertrophy. J Am Coll Cardiol 1993; 22: 1111-6.
7. Vardas PE, Simandirakis EN, Parthenakis FI, Manios EG, Eleftherakis NG, Terzakis DE. Study of late potentials and ventricular arrhythmias in hypertensive patients with normal electrocardiograms. Pacing Clin Electrophysiol 1994; 17: 577-84.
8. Perkiomaki JS, Ikaheimo MJ, Pikkujamsa SM, et al. Dispersion of the QT interval and autonomic modulation of heart rate in hypertensive men with and without left ventricular hypertrophy. Hypertension 1996; 28: 16-21.
9. Galinier M, Balanescu S, Fourcade J, et al. Prognostic value of ventricular arrhythmias in systemic hypertension. J Hypertens 1997; 15: 1779-83.
10. Han J, Moe GK. Nonuniform recovery of excitability in ventricular muscle. Circ Res 1964; 14: 44-60.
11. Kuo CS, Munakata K, Reddy CP, Surawicz B. Characteristics and possible mechanism of ventricular arrhythmia dependent on the dispersion of action potential durations. Circulation 1983; 67: 1356-67.
12. Hoekema R, Uijen GJH, Stilli D, van Oosterom A. Lead system transformation of body surface map data. J Electrocardiol 1998; 31: 71-82.
13. De Ambroggi L, AimŁ E, Ceriotti C, Rovida M, Negroni S. Mapping of ventricular repolarization potentials in patients with arrhythmogenic right ventricular dysplasia: principal component analysis of the ST-T waves. Circulation 1997; 96: 4314-8.
14. SippensGroenewegen A, Spekhorst H, van Hemel NM, et al. Body surface mapping of ectopic left and right ventricular activation: QRS spectrum in patients without structural heart disease. Circulation 1990; 82: 879-96.
15. Jackson JE. A user s guide to principal components. New York, NY: John Wiley & Sons, 1991.
16. De Ambroggi L, Negroni MS, Monza E, Bertoni T, Schwartz PJ. Dispersion of ventricular repolarization in the long QT syndrome. Am J Cardiol 1991; 68: 614-20.
17. Yamaki M, Ikeda K, Kubota I, et al. Improved diagnostic performance on the severity of left ventricular hypertrophy with body surface mapping. Circulation 1989; 79: 312-23.
18. Kornreich F, Montague TJ, Rautahariu PM, Kavadias M, Horacek MB, Taccardi B. Diagnostic body surface potential map patterns in left ventricular hypertrophy during PQRST. Am J Cardiol 1989; 63: 610-7.
19. Hirai M, Hayashi H, Ichihara Y, et al. Body surface distribution of abnormally low QRST areas in patients with left ven-

tricular hypertrophy. An index of repolarization abnormalities. Circulation 1991; 84: 1505-15.
20. Lux RL, Urie PM, Burgess MJ, Abildskov JA. Variability of the body surface distributions of QRS, ST-T and QRST deflection areas with varied activation sequence in dogs. Cardiovasc Res 1980; 14: 607-12.
21. Abildskov JA, Green LS, Evans AK, Lux RL. The QRST deflection area of electrograms during global alterations of ventricular repolarization. J Electrocardiol 1982; 15: 103-7.
22. Urie PM, Burgess MJ, Lux RL, Wyatt RF, Abildskov JA. The electrocardiographic recognition of cardiac states at high risk of ventricular arrhythmias. Circ Res 1978; 42: 350-8.
23. De Ambroggi L, Bertoni T, Locati E, Stramba-Badiale M, Schwartz PJ. Mapping of body surface potentials in patients with the idiopathic long QT syndrome. Circulation 1986; 74: 1334-45.
24. Gardner MJ, Montague TJ, Armstrong CS, Horacek BM, Smith ER. Vulnerability to ventricular arrhythmias: assessment by mapping of body surface potentials. Circulation 1986; 73: 684-92.
25. Mitchell LB, Hubley-Kozey CL, Smith ER, et al. Electrocardiographic body surface mapping in patients with ventricular tachycardia: assessment of utility in the identification of effective pharmacological therapy. Circulation 1992; 86: 383-93.
26. Yan GX, Antzelevitch C. Cellular basis for the normal T wave and the electrocardiographic manifestations of the long QT syndrome. Circulation 1998; 98: 1928-36.
27. Antzelevitch C, Shimitzu W, Yan GX, et al. The M cells: its contribution to the ECG and to normal and abnormal electrical function of the heart. J Electrophysiol 1999; 10: 1124-52.